

Spatio-temporal prediction of the population size at Tehran urban areas using BirnbaumSaunders Markov random fields

Majid Jafari Khaledi (✉ jafari-m@modares.ac.ir)

Tarbiat Modares University <https://orcid.org/0000-0002-2138-1098>

Sara Bourbour

Tehran Center for Urban Statistics and Observatory

Helia Safarkhanloo

Tehran Center for Urban Statistics and Observatory

Research Article

Keywords: Skewed spatial data, Birnbaum-Saunders distribution, Markov random field, Population rate, Census data, Bayesian Inference

Posted Date: October 15th, 2021

DOI: <https://doi.org/10.21203/rs.3.rs-958268/v1>

License:  This work is licensed under a Creative Commons Attribution 4.0 International License.

[Read Full License](#)

Spatio-temporal prediction of the population size at Tehran urban areas using Birnbaum-Saunders Markov random fields

Majid Jafari Khaledi¹

Department of Statistics, Tarbiat Modares University, Tehran Iran. Email: jafari-m@modares.ac.ir

Sara Bourbour

Head of Tehran Center for Urban Statistics and Observatory. Email: sara.burbur@gmail.com

Helia Safarkhanloo

Employee of Tehran center for Urban Statistics and Observatory. Email: heliasafarkhanloo@gmail.com

Abstract

For implementing an intelligent urban management, it is necessary and inevitable to know the population size in different areas of Tehran city and identify how they change over time. Population and housing census data can determine the spatio-temporal distribution of the people and how it evolves. However, census will not be implemented across the country in 2021, like a previous manner, due to issues related to the coronavirus pandemic and its prevalence. From this perspective, the prediction of the population size is significant in different regions of Tehran for the year 2021. This paper focuses on developing a statistical learning model for predicting the population growth rate of Tehran urban areas. To be more specific, since the growth rates data are spatially correlated, skewed to the right, and positive, a Birnbaum- Saunders Markov random field (BSMRF) is proposed. We adopt a Bayesian framework for the parameter estimation and spatial prediction and use Markov chain Monte Carlo methods to sample from the posterior distribution. Then, the results are compared with the traditional models.

Keywords: Skewed spatial data, Birnbaum-Saunders distribution, Markov random field, Population rate, Census data, Bayesian Inference.

1. Introduction

One of the most critical indicators of Tehran's relations is the spatial distribution of the population and how it has evolved; this is also known as population foresight or future foresight. Tehran has become the 24th most populous city in the world. A city currently faces many biological problems and faces various crises such as pollution, climate, traffic, etc. This city involves 22 urban areas. The placement of four new cities on the edge of Tehran has created the need to provide more than 15 million people. Table 1 shows the population of Tehran and the annual population growth in

¹ Corresponding Author

1986-2016 based on censuses. According to Figure 1, Tehran's population growth had declined sharply from 2.9% in 1986, and this amount has reached its minimum in recent years. Tehran is one of the most populous metropolises in Iran. One of the reasons for this decrease in population in Tehran could be the high cost of living in this city, especially the high cost of housing. The excess population of this city migrated to the suburbs. In 1956, about 95% of the urban population of Tehran province lived in Tehran. While in 2016, the city of Tehran accommodates about 70% of the province's urban population. The 1956 census is the first general census of the country's population, in which all people in the country were counted. The year 1956 can be considered the beginning of systematic and scientific population censuses in the country. In 2006, according to the Tehran city council, the gap between the implementation of general censuses of population and housing decreased from ten years to five years. Therefore, according to the last census conducted in 2016, 2021 is the available census of population and housing. Unfortunately, due to coronavirus issues, there will be no census in 2021. Coronavirus pandemic has affected Iran extensively.

Table 1- Population of Tehran and population growth rate from 1986 to 2016.

| Year | Population | Annual growth |
|-------------|-------------------|----------------------|
| 1986 | 6,042,584 | 2.9 |
| 1996 | 6,758,845 | 1.1 |
| 2006 | 7,803,883 | 1.4 |
| 2011 | 8,154,051 | 0.9 |
| 2016 | 8,679,936 | 1.26 |

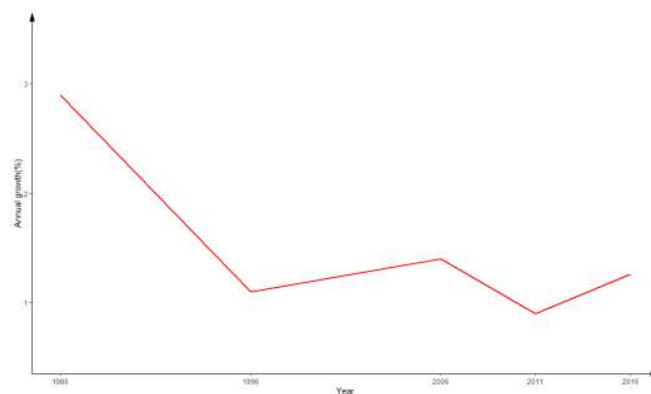


Figure 1- The population growth rate at Tehran city from 1986 to 2016.

This main motivation of this study is to provide spatio-temporal prediction of the population size at Tehran urban areas for the year 2021. According to some reports and empirical researches, the population growth rate between 2016 and 2021 can be considered relatively equal to that between 2011 and 2016. The main contribution of this paper is to develop a new Markov random field based on the Birnbaum-Saunders distribution for the population growth rate between 2011 and 2016. The motivating feature of this modeling framework is that it incorporates positive, skewed to the right and spatially correlated data, as needed in many empirical circumstances. Hence, the methodology presented here makes new research for modeling skewed spatial data.

A spatial process observed over a network is usually modeled using a traditional Gaussian Markov random field (GMRF) where the spatial dependence between data is captured based on a precision matrix corresponding to a labelled graph. A nice feature of the GMRF's is conditional independence property. This feature brings sparsity of the precision matrix enabling the network to benefit from computation. Accordingly, this technique has an important role in machine learning. The required background and application in machine learning contexts, are given, for example, in Gelfand et al. (2010), Banerjee et al. (2014), Siden and Lindsten (2020), Perdikaris et al. (2015). However, Gaussianity assumption might be overly restrictive to represent the data. The real data could be highly non-Gaussian and may show features like skewness. In the case of point reference data, various approaches have been provided in the literature to handle this problem, including transformed Gaussian random fields (De Oliveira, et al. 1997), skew-Gaussian processes (Zhang and El-Shaaravi, 2010; Zareifard and Jafari Khaledi, 2013; Rimstad and Omre, 2014, Zareifard et al., 2018), Tukey g-and-h process (Xu and Genton, 2017; Yan and Genton, 2017), Birnbaum-Saunders (BS) model (Garcia-Papani et al. 2017, 2018), copula models (Bárdossy and Li, 2008; Kazianka and Pilz, 2009; Pilz et al., 2008; Kazianka and Pilz, 2010; Krupskii and Genton, 2017; Prates et al., 2015; Krupskii et al., 2018) and convolution of log-Gaussian and Gaussian processes (Zareifard et al., 2018, 2019). However, there is little work to be done in skewness modeling for spatial areal data. To reduce unrealistic assumptions for conditional autoregressive models, Prates et al. (2014) considered a non-Gaussian distribution for the random effects in spatial generalized linear mixed models where incorporates skewness as well as heavy tail behavior of the data. However, although the covariance matrix of their random effects depends on its neighbors, the Markov property does not supported. Also, for the class of autoregressive and moving average (ARMA) models, Pourahmadi (2007) studied the construction of stationary skew normal ARMA models for colored skew normal noise.

The aim of this paper is to introduce a novel non-Gaussian Markov random field using the Birnbaum-Saunders distribution (Birnbaum and Saunders, 1969a and 1969b). After investigating the main probabilistic features involving the conditional independence of the introduced random field, the focus of the paper is on the Bayesian approach to carry out statistical inference. We also develop and implement a Markov chain Monte Carlo (MCMC) sampling strategy for posterior computations, which is found to work quite well. There are strong connections between our approach and the method in Garcia-Papani et al. (2017 and 2018). In particular, these works introduce a Birnbaum-Saunders spatial regression model, while we develop a new Markov random field for the areal data. However, their framework can only be applied for point-referenced data settings.

The rest of the paper is organized as follows. In the following section, a brief description and summary of the data, along with the motivation of considering a skewed spatial model, is provided. Section 3 introduces the new class of skewed spatial models and also discusses the Bayesian analysis of the model. Application to the data from Tehran is presented in Section 4. Finally, in Section 5 we present some conclusions and final remarks.

2. Population growth rate data

The data used for this study is collected from Statistical Centre of Iran and provided from Center for Urban Statistics and Observatory. Our data include the population growth rate between 2011 and 2016 at 22 Tehran urban regions. From the population division below area i in the last census to the population of the same area in the previous census, the dependent variable is made. The last census is the 2016 census, and the pre-last census is the 2011 census. The evidence of spatial correlation is confirmed through Figure 2 where we show the population growth rate spread in all the urban regions. The map depicts that the regions with high rate are closer together and same can be said about regions with low rate. This gives us strong evidence for spatial correlation in the population growth rate data. Given this, the use of classical models for data analysis does not seem justified. According to the figure, the region 22 has the highest, and the region 13 has the lowest population growth rate between 2011 and 2016. For further research, the Moran's I test is used to examine spatial correlation. The value of this statistic was 0.46, which indicates a high level of spatial correlation between the data.

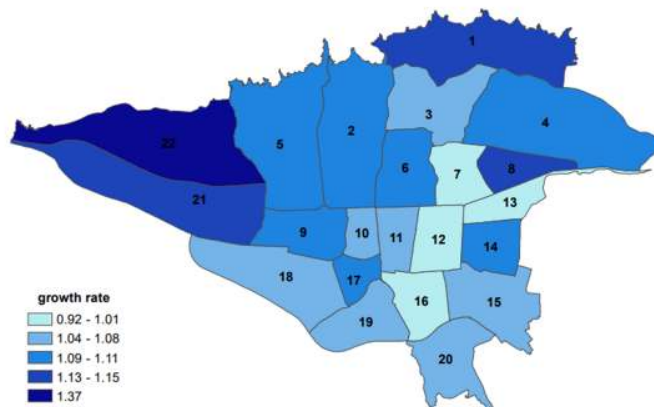


Figure 2. The population growth rate between 2011 and 2016 in urban regions of Tehran.

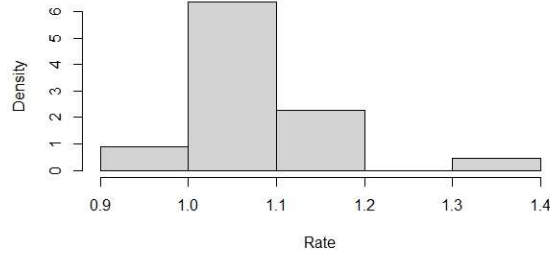


Figure 3. Histogram of the data.

Therefore, the data can be modeled using a Gaussian–Markov random field model. However, the histogram of data (Figure 3) suggests that the data have a right-skewed distribution and hence motivates us for creating an appropriate skewed spatial model. With regard to use of covariate information can significantly increase prediction accuracy, after studying different variables and studying their correlation with the response variable, four covariates including death count, number of families, number of elderly, and children in different regions were selected and considered in the model in a regression framework.

3. Methodology

3.1 Birnbaum Saunders Markov random field (BSMRF)

Consider a grid containing n areas of $1, \dots, n$ with neighboring system $N(k)$, $k=1, \dots, n$. Suppose $Z=(Z_1, \dots, Z_n)$ displays latent variable values in n regions. Following the general GMRF model proposed by Ferreira and Di Oliveira (2007), we assume that this random vector follows a Gaussian Markov random field, i.e. the joint distribution of the random vector is

$$Z \sim N_n(0, \Sigma_\phi) \quad (1)$$

with the precision matrix $\Sigma_\phi^{-1} = (I_n + \phi H)$, where the parameter $\phi \geq 0$, controls the dependency intensity between the Z vector components and I_n is the $n \times n$ identity matrix. The matrix H assumed known, allows the modeling of different patterns of spatial association by the specification of different neighborhood systems and

$$(H)_{kl} = \begin{cases} h_k, & k = l \\ -g_{kl}, & k \in N(l) \\ 0, & o.w \end{cases} \quad (2)$$

where $g_{kl} > 0$ shows a measure of similarity between regions k region and l , so that $g_{kl} = g_{lk}$, and $h_k = \sum_{l \in N(k)} g_{kl}$. Accordingly, the matrix Σ_ϕ^{-1} is symmetry and diagonally dominant and so it is also positive definite (Ferreira and De Oliveira, 2007). The model (1) can also be expressed based on the following full conditional distributions

$$Z_k | Z_l, l \in N(k) \sim N \left(\frac{\phi \sum_{l \in N(k)} g_{kl} Z_l}{1 + \phi h_k}, \frac{1}{(1 + \phi h_k)} \right), k = 1, \dots, n \quad (3)$$

Now, define a random vector $\boldsymbol{\eta} = (\eta_1, \dots, \eta_n)$ through

$$\begin{aligned}\eta_i &= \left(\frac{\alpha Z_i}{2} + \sqrt{\left(\frac{\alpha Z_i}{2}\right)^2 + 1} \right)^2 \\ &= \exp \left(2 \operatorname{arc} \sinh \left(\frac{\alpha Z_i}{2} \right) \right).\end{aligned}$$

Then, each η_i marginally has a Birnbaum-Saunders distribution $\text{BS}(1, \alpha)$ with the probability density function

$$f_{\eta_i}(t; \alpha) = \frac{1}{2\sqrt{2\pi}\alpha} \left(\sqrt{\frac{1}{t}} + \sqrt{\frac{1}{t^3}} \right) \exp \left\{ -\frac{1}{2\alpha} \left(t + \frac{1}{t} - 2 \right) \right\}, \quad t > 0, \alpha > 0.$$

The shape parameter α controls the skewness coefficient of the distribution. We call $\boldsymbol{\eta}$ a Birnbaum-Sanders Markov random field and denoted by $\text{BSMRF}(\alpha, \Sigma_\phi)$. It is completely specified by the shape parameter α and a correlation matrix Σ_ϕ as follows:

$$f_{\boldsymbol{\eta}}(\mathbf{t}; \alpha, \Sigma_\phi) = \phi_n(\mathbf{w}; \Sigma_\phi) \times \prod_{i=1}^n \frac{1}{2\alpha} \left(\sqrt{\frac{1}{t_i}} + \sqrt{\frac{1}{t_i^3}} \right),$$

such that $\mathbf{w} = 1/\alpha \left(\left(\sqrt{t_1} - \frac{1}{\sqrt{t_1}} \right), \dots, \left(\sqrt{t_n} - \frac{1}{\sqrt{t_n}} \right) \right)$ and $\phi_n(\mathbf{w}; \Sigma_\phi)$ denotes the density function of $N_n(\mathbf{0}, \Sigma_\phi)$. Note that matrix Σ_ϕ is not the correlation matrix of $\boldsymbol{\eta}$ and that the BSMRF is not affected by the scales of the original GMRF. According to De Oliveira (2013), the covariance between η_i and η_j is

$$\operatorname{Cov}(\eta_i, \eta_j) = \sum_{k=1}^{\infty} a_k^2 \frac{\Sigma_\phi(i, j)^k}{k!},$$

where $a_k = \int_{-\infty}^{+\infty} g(t) H_k(t) \phi(t) dt$, $g(t) = \left(\frac{\alpha t}{2} + \sqrt{\left(\frac{\alpha t}{2}\right)^2 + 1} \right)^2$, $\phi(t)$ is the pdf of the standard normal distribution. As usually used for GMRFs, we can present a BSMRF using the precision matrix $Q = \Sigma_\phi^{-1}$. This leads to an intuitive interpretation of conditional distributional properties. Since the transformations are marginal-wise, the Markov property is inherited by the BSMRF. To be more specific, we have

$$\eta_i \perp \eta_j | \eta_{(-ij)} \text{ for } i \neq j \text{ if and only if } Q_{ij} = 0,$$

where $\eta_{(-ij)}$ is $\boldsymbol{\eta}$ without the i th and j th observations. The sparseness of the precision matrix Q completely specifies the graph of the BSMRF and, hence, its conditional dependence structure. For convenience, we denote a BSMRF with the shape parameter α and precision matrix Q in the

original scale by $\text{BSMRF}(\alpha, Q)$. Note that matrix Q is not the precision matrix of $\boldsymbol{\eta}$ and that the BSMRF is not affected by the scales of the original GMRF.

3.2 Spatial mixed effects model

Suppose that we observe (Y_i, \mathbf{X}_i) at sites $i = 1, \dots, n$, where Y_i is the response variable and \mathbf{X}_i a $q \times 1$ covariate vector. Let $\mathbf{Y} = (Y_1, \dots, Y_n)$ and $\mathbf{X} = (\mathbf{X}_1, \dots, \mathbf{X}_n)'$. The response variable is assumed to have the following mixed effect model representation:

$$\text{Data Model: } \ln(Y_i) = S_i + \epsilon_i, \quad (4)$$

$$\text{Process Model: } S_i = \mu_i + \ln(\eta_i), \quad (5)$$

where S_i represents the spatial latent process, $\epsilon_i \sim N(0, \tau^2)$ represents measurement error, $\mu_i = \mathbf{X}_i' \boldsymbol{\beta}$ is a deterministic mean function with a p -dimensional vector of unknown regression coefficients $\boldsymbol{\beta}$ and $\boldsymbol{\eta} = (\eta_1, \dots, \eta_n) \sim \text{BSMRF}(\alpha, Q)$. The stochastic components η_i and ϵ_i are assumed independent. Note that the spatial latent process S_i follows a log-Birnbaum-Sanders distribution with shape parameter α and location parameter μ_i . We write $\mathbf{S} = (S_1, \dots, S_n) \sim \text{log} - \text{BSMRF}(\boldsymbol{\beta}, \alpha, Q)$. In this case,

$$f_{\mathbf{S}}(\mathbf{s}; \boldsymbol{\beta}, \alpha, \Sigma_{\phi}) = (2\pi)^{-\frac{n}{2}} |Q|^{\frac{1}{2}} \exp\left\{-\frac{1}{2} \mathbf{z}' Q \mathbf{z}\right\} \times \prod_{i=1}^n \frac{1}{\alpha} \cosh\left(\frac{S_i - \mu_i}{2}\right),$$

where $\mathbf{z} = \frac{2}{\alpha} \left(\sinh\left(\frac{S_1 - \mu_1}{2}\right), \dots, \sinh\left(\frac{S_n - \mu_n}{2}\right) \right)$. Based on the spectral analysis, the symmetric matrix H can be written as $H = PDP'$, where P has orthogonal columns for the normalized vectors of the matrix H and $D = \text{diag}(\lambda_1, \dots, \lambda_n)$ is a diagonal matrix for the ordered values of H in the form $\lambda_1 \geq \dots \geq \lambda_{n-1} > \lambda_n = 0$. Therefore:

$$\begin{aligned} |Q| &= |\phi PDP' + I_n| = |\phi P'PD + I_n| \\ &= |\phi D + I_n| = \left| \phi \times \begin{pmatrix} \lambda_1 & \dots & 0 \\ 0 & \dots & 0 \\ 0 & \dots & \lambda_n \end{pmatrix} + \begin{pmatrix} 1 & \dots & 0 \\ 0 & \dots & 0 \\ 0 & \dots & 1 \end{pmatrix} \right| \\ &= \left| \begin{pmatrix} \phi\lambda_1 + 1 & \dots & 0 \\ 0 & \dots & 0 \\ 0 & \dots & 1 \end{pmatrix} \right| = \prod_{k=1}^{n-1} (\phi\lambda_k + 1). \end{aligned} \quad (6)$$

In summary, a hierarchical model with a BSMRF component for the spatial latent process, is of the form

$$\begin{aligned} Y_i | S_i &\sim \text{log-N}(S_i, \tau^2), \quad i = 1, \dots, n, \\ \mathbf{S} = (S_1, \dots, S_n) &\sim \text{log} - \text{BSMRF}(\boldsymbol{\beta}, \alpha, Q). \end{aligned}$$

The model parameters of interest are $\boldsymbol{\theta} = (\boldsymbol{\beta}, \alpha, \tau^2, \phi)$.

3.3 Bayesian analysis

In the following, the Bayesian inference of the proposed model will be offered. We complete the hierarchy of the model by specifying the prior distribution for the vector of the model parameters. The components of the parameter vector were initially assumed to be independent a priori. Then, proper prior distributions were assigned to the parameters. Accordingly, the joint posterior density of $\boldsymbol{\theta}$ and \boldsymbol{S} is:

$$\pi(\boldsymbol{\theta}, \boldsymbol{S} | \boldsymbol{Y}) \propto \left[\prod_{i=1}^n \pi(y_i | s_i) \right] f_{\boldsymbol{S}}(\boldsymbol{s}; \boldsymbol{\beta}, \alpha, \Sigma_{\phi}) \pi(\boldsymbol{\beta}) \pi(\alpha) \pi(\tau^2) \pi(\phi). \quad (7)$$

In our study, the prior distributions of $\boldsymbol{\beta}$ and τ^2 were set to be conjugate normal and inverse gamma distributions, respectively. The hyperparameters are chosen in the way that the corresponding prior distributions to be vague. The prior distribution of the shape parameter α was set to be $\Gamma(\kappa_1, \kappa_2)$, a gamma distribution with shape κ_1 and scale κ_2 . The hyperparameters were set to be $\kappa_1 = 0.01$ and $\kappa_2 = 100$. These priors were chosen to be proper but vague to allow the posterior estimates to be mainly data driven. A uniform prior over $(0, 1)$ was put on the dependence parameter ϕ to ensure positive spatial dependence as intuitively expected (Banerjee et al., 2014). A general Gibbs sampling algorithm with Metropolis–Hasting update can be devised to draw from $\pi(\boldsymbol{\theta}, \boldsymbol{S} | \boldsymbol{Y})$. Since the quantile function of the log-Birnbaum-Saunders distribution can be written in BUGS, an implementation of the proposed model would be very easy.

4. Analysis of experimental data

We fitted three models to the population growth data: the GMRF model, the log-GMRF model, and BSMRF model. An intercept model with the available covariates were fit for each model where any two regions within 10 km were considered to be neighbors. For each model, two chains with 10,000 iterations each were generated. We discarded the first 5,000 iterations as burn-in and thinned the rest by 5, resulting in 1,000 posterior samples. Convergence was verified using Gelman and Rubin (1992) criteria. To compare different models for the same data, we propose to use the conditional predictive ordinate (CPO) criterion (e.g., Gelfand et al., 1992; Dey et al., 1997). The summary statistic is the logarithm of the pseudo-marginal likelihood (LPML), which is the summation of the log density of leave-one-out marginal predictive posterior distribution. Notice that a higher value of the LPML indicates a better fit of the model.

The BSMRF model had the largest LPML (−394.92), followed by the log-GMRF model (−401.17) and the GMRF model (−428.03). These results suggest that the BSMRF model provides considerably better fit than did the traditional GMRF model and the log-GMRF model. This difference is quite strong evidence in favor of the BSMRF model over the GMRF model. The posterior point estimates and 95% confidence

| | Mean | SD | val2.5pc | median | val97.5pc |
|-------|----------|--------|----------|----------|-----------|
| Alpha | 0.3032 | 0.1917 | 0.03824 | 0.2735 | 0.6953 |
| beta0 | 0.2232 | 0.2691 | -0.1418 | 0.1531 | 0.9457 |
| beta1 | -0.01801 | 0.1759 | -0.3958 | 0.00359 | 0.3137 |
| beta2 | 0.1755 | 0.1832 | -0.05908 | 0.1356 | 0.6464 |
| beta3 | 0.1989 | 0.2064 | -0.157 | 0.1794 | 0.6533 |
| beta4 | 0.07644 | 0.1509 | -0.2576 | 0.08604 | 0.3767 |
| S[1] | 0.2233 | 0.2749 | -0.3095 | 0.2158 | 0.7491 |
| S [2] | 0.115 | 0.2607 | -0.385 | 0.1094 | 0.6724 |
| S [3] | 0.09968 | 0.3279 | -0.5528 | 0.1069 | 0.7359 |
| S [4] | 0.05154 | 0.1772 | -0.2793 | 0.05157 | 0.3925 |
| S[5] | -0.0417 | 0.2163 | -0.4967 | -0.02346 | 0.3704 |
| S[6] | 0.1564 | 0.2936 | -0.4256 | 0.1505 | 0.8152 |
| S[7] | -0.114 | 0.2528 | -0.7076 | -0.08643 | 0.3372 |
| S[8] | 0.02952 | 0.2328 | -0.4723 | 0.04417 | 0.477 |
| S[9] | 0.0111 | 0.2085 | -0.4098 | 0.01224 | 0.4559 |
| S[10] | 0.05461 | 0.1934 | -0.3257 | 0.07312 | 0.4327 |
| S[11] | -0.06451 | 0.1863 | -0.4233 | -0.06603 | 0.3351 |
| S[12] | 0.06436 | 0.3216 | -0.5707 | 0.094 | 0.6242 |
| S[13] | -0.2385 | 0.3184 | -0.9344 | -0.1992 | 0.3284 |
| S[14] | 0.149 | 0.2613 | -0.3093 | 0.1298 | 0.7325 |
| S[15] | -0.05137 | 0.2018 | -0.4056 | -0.06257 | 0.3982 |
| S[16] | -0.08832 | 0.2882 | -0.6201 | -0.07891 | 0.4816 |
| S[17] | -0.02806 | 0.279 | -0.6172 | -0.01853 | 0.593 |
| S[18] | 0.06764 | 0.2415 | -0.3925 | 0.07138 | 0.5318 |
| S[19] | -0.08148 | 0.2751 | -0.5767 | -0.08163 | 0.5085 |
| S[20] | 0.02833 | 0.1884 | -0.3225 | 0.02557 | 0.441 |
| S[21] | 0.1398 | 0.4616 | -0.8237 | 0.1878 | 1.038 |
| S[22] | 0.2725 | 0.5257 | -0.907 | 0.2989 | 1.164 |

Table 2- Posterior point estimates, standard deviations (SD) and 95% confidence intervals of the parameters and the spatial latent variables in the BSMRF regression model. The regression coefficients are in the order of intercept, the rate of deaths, the rate of elderly, the rate of households, and the rate of children below 15.

intervals of the parameters and the spatial latent process from the BSMRF model are summarized in Table 2. Neither covariates was found to have a significant effect on the population growth rate. Table 3 shows the predicted values of the population in 22 urban regions. Figure 4 also displays the prediction map of the population size in 2021.

| Region | Predicted Population |
|--------|----------------------|
| 1 | 617,458 |
| 2 | 776,986 |
| 3 | 364,594 |
| 4 | 965,776 |
| 5 | 821,581 |
| 6 | 293,204 |
| 7 | 278,386 |
| 8 | 437,778 |
| 9 | 176,058 |
| 10 | 345,233 |
| 11 | 288,923 |
| 12 | 256,924 |
| 13 | 199,358 |
| 14 | 567,686 |
| 15 | 626,447 |
| 16 | 245,051 |
| 17 | 270,652 |
| 18 | 448,588 |
| 19 | 235,538 |
| 20 | 378,163 |
| 21 | 214,275 |
| 22 | 230,340 |

Table 3. Population size of the urban regions in 2021.

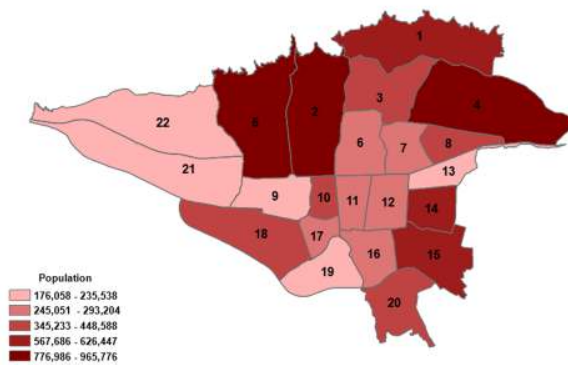


Figure 4. The Prediction map of population in 2021 at Tehran under BSMRF model.

5. Discussion and Conclusion

In spatial random effects models, the random effects are priori assumed to have a normal distribution, which may not be a valid assumption. Although various approaches have been provided in the literature to handle this problem, we provided a new approach to deal with skewed spatial areal data. A Gibbs algorithm was developed for the Bayesian inference. The applied

example illustrated the methodology and its utility in practice. According to the findings, the proposed model has an appropriate ability to provide a more precise prediction than the GMRF model. The LMPL shows that the predictive performance of the BSMRF model compares favorably with GMRF and Log-GMRF models.

It is also worth noting that the model considered in this research has the potential to be used in other modelling frameworks such as the generalized linear spatial models. To save time, our proposed approach can also be extended to provide fully model-based inference large datasets. These issues will be studied in future works.

References

- Banerjee, S., Carlin, B. P., and Gelfand, A. E. (2014). Hierarchical modeling and analysis for spatial data, Boca Raton, FL: Chapman and Hall/CRC.
- Bardossy, A., and Li, J. (2008). Geostatistical interpolation using copulas. *Water Resources Research*, 44(7).
- Birnbaum, Z. W., and Saunders, S. C. (1969a). A new family of life distributions. *Journal of applied probability*, 6(2), 319-327.
- Birnbaum, Z. W., and Saunders, S. C. (1969b). Estimation for a family of life distributions with applications to fatigue. *Journal of Applied Probability*, 6(2), 328-347.
- De Oliveira, V., Kedem, B., and Short, D. A. (1997). Bayesian prediction of transformed Gaussian random fields. *Journal of the American Statistical Association*, 92(440), 1422-1433.
- Dey, D.K., Chen, M.H., Chang, H., (1997). Bayesian approach for nonlinear random effects models. *Biometrics* 53, 1239–1252.
- Ferreira, M. A., and De Oliveira, V. (2007). Bayesian reference analysis for Gaussian Markov random fields. *Journal of Multivariate Analysis*, 98(4), 789-812.
- Garcia-Papani, F., Uribe-Opazo, M. A., Leiva, V., and Aykroyd, R. G. (2017). Birnbaum Saunders spatial modelling and diagnostics applied to agricultural engineering data. *Stochastic Environmental Research and Risk Assessment*, 31(1), 105-124.
- Garcia-Papani, F., Leiva, V., Uribe-Opazo, M. A., and Aykroyd, R. G. (2018). Birnbaum-Saunders spatial regression models: Diagnostics and application to chemical data. *Chemometrics and Intelligent Laboratory Systems*, 177, 114-128.
- Gelfand, A. E., Dey, D. K., and Chang, H. (1992). Model determination using predictive distributions with implementation via sampling-based methods. *Bayesian Statistics*, 4, 147-167.

- Gelfand, A. E., Diggle, P., Guttorp, P., and Fuentes, M. (Eds.). (2010). Handbook of spatial statistics. CRC press.
- Gelman, A., and Rubin, D. B. (1992). Inference from iterative simulation using multiple sequences. *Statistical Science*, 7(4), 457-472.
- Kazianka, H., and Pilz, J. (2009). A corrected criterion for selecting the optimum number of principal components. *Austrian Journal of Statistics*, 38(3), 135-150.
- Kazianka, H., and Pilz, J. (2010). Copula-based geostatistical modelling of continuous and discrete data including covariates. *Stochastic Environmental Research and Risk Assessment*, 24(5), 661-673.
- Krupskii, P., and Genton, M. G. (2017). Factor copula models for data with spatio-temporal dependence. *Spatial Statistics*, 22, 180-195.
- Krupskii, P., Huser, R., and Genton, M. G. (2018). Factor copula models for replicated spatial data. *Journal of the American Statistical Association*, 113(521), 467-479.
- Perdikaris, P., Venturi, D., Royset, J. O., & Karniadakis, G. E. (2015). Multi-fidelity modelling via recursive co-kriging and Gaussian–Markov random fields. *Proceedings of the Royal Society A: Mathematical, Physical and Engineering Sciences*, 471(2179), 20150018.
- Pilz, J., Kazianka, H., and Spock, G. (2008). Interoperability-spatial interpolation and automated mapping. In: Tsiligiridis T (ed) *Proceedings of the 4th international conference on information and communication technologies in bio and earth sciences HAICTA*. Agricultural University of Athens, 110-118
- Pourahmadi, M. (2007). Skew-normal ARMA models with nonlinear heteroscedastic predictors. *Communications in Statistics—Theory and Methods*, 36(9), 1803-1819.
- Prates, M. O., Costa, D. R., & Lachos, V. H. (2014). Generalized linear mixed models for correlated binary data with t-link. *Statistics and Computing*, 24(6), 1111-1123.
- Prates, M. O., Dey, D. K., Willig, M. R., and Yan, J. (2015). Transformed Gaussian Markov random fields and spatial modeling of species abundance. *Spatial Statistics*, 14, 382-399.
- Rimstad, K., Omre, H. (2014). Skew-Gaussian random fields. *Spatial Statistics*, 10, 43-62.
- Sidén, P., and Lindsten, F. (2020). Deep gaussian markov random fields. In *International Conference on Machine Learning* (pp. 8916-8926). PMLR.
- Xu, G., and Genton, M. G. (2017). Tukey g-and-h random fields. *Journal of the American Statistical Association*, 112(519), 1236-1249.
- Yan, Y., and Genton, M. G. (2017). Non-Gaussian autoregressive processes with Tukey g-and-h transformations. *Environmetrics*, e2503.
- Zareifard, H., and Jafari Khaledi, M. (2013). Non-Gaussian modelling of spatial data using scale mixing of a unified skew Gaussian process. *Journal of Multivariate Analysis*, 114, 16-28.

Zareifard, H., Jafari Khaledi, M., Rivaz, F., and Vahidi-Asl, M. Q. (2018). Modelling skewed spatial data using a convolution of Gaussian and log-Gaussian processes. *Bayesian Analysis*, 13(2), 531-557.

Zareifard, H., Jafari Khaledi, M., and Dahdouh, O. (2019). Multivariate spatial modelling through a convolution-based skewed process. *Stochastic Environmental Research and Risk Assessment*, 33, 657-671.

Zhang, H., and El-Shaarawi, A. (2010). On spatial skew-Gaussian processes and applications. *Environmetrics*, 21(1), 33-47.